Using satellite data to estimate partial pressure of CO2 in the Baltic Sea

Gaëlle Parard, Anastase Alexandre Charantonis, Anna Rutgersson

AGU PUBLICATIONS

JGR

Journal of Geophysical Research: Biogeosciences

RESEARCH ARTICLE
10.1002/2015JG003064

Key Points:
- Evolution of the pCO_2 from 1998 to 2011
- The self-organizing multiple linear output (SOMLO) method from the remotely sensed measures
- The seasonal variability in the Baltic Sea, being high in winter and low in summer

Correspondence to:
G. Parard,
parard.gaelle@gmail.com

Citation:
Parard, G., A. A. Charantonis, and A. Rutgersson (2016), Using satellite data to estimate partial pressure of CO_2 in the Baltic Sea, *J. Geophys. Res. Biogeosci*, *121*, 1002–1015, doi:10.1002/2015JG003064.

Received 15 JUN 2015
Accepted 4 MAR 2016
Accepted article online 10 MAR 2016
Published online 31 MAR 2016

Using satellite data to estimate partial pressure of CO_2 in the Baltic Sea

Gaëlle Parard[1], Anastase Alexandre Charantonis[2,3], and Anna Rutgersson[1]

[1]Department of Earth Sciences, Uppsala University, Uppsala, Sweden, [2]Centre d'études et de recherche en Informatique, Conservatoire des Arts et Metiers, Paris, France, [3]Laboratoire d'Océanographie et du Climat : Expérimentations et Approches Numeriques, Université Pierre et Marie Curie, Paris, France

Abstract In this study we focused on estimating the pressure partial of CO_2 (pCO_2) in the entire Baltic Sea which can be considered a coastal area in its entirety. We used the self-organizing multiple linear output (SOMLO) method to estimate the ocean surface pCO_2 in the Baltic Sea from the remotely sensed sea surface temperature, chlorophyll *a*, colored dissolved organic matter, net primary production, and mixed-layer depth. Uncertainties in the estimates include sparsity of in situ data used to train the algorithms, in particular, for some sectors and seasons. For this application we divided the Baltic Sea in four basins. When comparing the results obtained with this division to those obtained in previous studies, we notice a decrease in the root-mean-square error (<40 μatm) between the reconstruction of the pCO_2 and their corresponding in situ measurements, as well as an increase of the correlation coefficient (> 0.96) between them. The outputs of this research have a horizontal resolution of 4 km and cover the 1998–2011 period. For the first time, a climatological mean distribution of surface water pCO_2 over the Baltic Sea was calculated based on the SOMLO method with a mean pCO_2 of 368.3 ± 100 μatm, and a range of 234–514 μatm. The seasonal variability is similar throughout the Baltic Sea, being high in winter and low in summer.

1. Introduction

The concentration of carbon dioxide (CO_2) in the atmosphere is steadily increasing because of human activities such as fossil fuel burning [*Stocker et al.*, 2013]. To understand how this is affecting the planet, several pieces of knowledge of the CO_2 system have to be investigated. Therefore, understanding how the ocean modulates atmospheric CO_2 is important because the ocean absorbs up to one third of anthropogenic CO_2 emissions, according to in situ data and model output [e.g., *Wanninkhof et al.*, 2013]. Although our grasp of the global air-sea CO_2 flux has improved in recent years, large uncertainties remain, particularly when increasing the spatial and temporal scale. One important type of region is the coastal seas, which have been continuously used by people and strongly influenced by industrialization. Coastal environments represent 7.6% of the total oceanic surface area [*Sverdrup et al.*, 1942]; they are, however, biogeochemically more dynamic and probably more vulnerable to climate change than the open ocean. There are uncertainties as to the role of coastal oceans in the global carbon cycle, and *Tsunogai et al.* [1999], supported by observations, demonstrated the removal of a significant amount of pCO_2 from the atmosphere (i.e., 55 μatm) in the shelf region of the East China Sea. The hypothesis is that if the world continental shelf zone absorbs atmospheric CO_2 at the same rate as the East China Sea, the uptake from the atmosphere would represent 1 Pg C yr^{-1}. Such a sink is comparable to the open ocean sink of atmospheric CO_2, which is estimated to be 1.4 Pg C yr^{-1} [*Borges*, 2011]. More recently, *Laruelle et al.* [2014] demonstrated that the coastal oceans are a much smaller CO_2 sink than was previously thought, i.e., 0.2 Pg C yr^{-1}. Whatever the responses of the open ocean to climate change, they will propagate to the coastal ocean. Superimposed on this background open oceanic forcing, the coastal ocean will also respond to changes in fluxes from the land biosphere via rivers, groundwaters, and atmospheric deposition of major biogeochemical elements (e.g., carbon, nitrogen, phosphorous, and silica) in organic and inorganic forms. Physical settings specific to the coastal ocean (e.g., coastal upwelling and sea ice) are also expected to respond to climate change, probably leading to unique and local changes in carbon cycling [*Frankignoulle and Borges*, 2001; *Gattuso et al.*, 1998; *Borges et al.*, 2005].

To address this problem, the research community that studies open ocean fluxes of CO_2 has devised various schemes for estimating surface pCO_2.

The most common scheme has been to use sea surface temperature (SST) to predict pCO_2 [e.g., *Lee et al.*, 1998; *Lefèvre and Taylor*, 2002]. SST-pCO_2 relationships tend to be robust in nearly all ocean regions [*Lee et al.*, 1998] because the two parameters usually covary closely. This is partly because of the direct thermodynamic effect of SST on pCO_2 discussed by *Takahashi et al.* [1993] and also because SST is a strong tracer of mixing and under certain circumstances influences biological productivity. However, in the past decade, several authors have reported the application of a neural network technique to basin-scale pCO_2 sea analysis [*Lefévre et al.*, 2005; *Jamet et al.*, 2007; *Friedrich and Oschlies*, 2009; *Telszewski et al.*, 2009; *Landschützer et al.*, 2013; *Nakaoka et al.*, 2013; *Schuster et al.*, 2013], concentrating mainly on the North Atlantic Ocean.

The advent of readily available satellite-derived SST products and their obvious spatiotemporal advantages has fueled interest in remote sensing approaches to pCO_2 estimation. *Stephens et al.* [1995] pioneered this approach when they used satellite SST data to predict pCO_2 in the North Pacific, and similar approaches have since been applied to the Greenland Sea gyre [*Hood and Merlivat*, 2001], the Sargasso Sea [*Nelson et al.*, 2001], the North Atlantic in winter [*Olsen et al.*, 2003], and the Caribbean Sea [*Olsen et al.*, 2004].

Unfortunately, pCO_2-SST relationships fail in some situations, usually related to high biological activity: *Stephens et al.* [1995] found that their pCO_2-SST relationship did not work well in the biologically productive northwest North Pacific, *Olsen et al.* [2003] found that the impact of the spring bloom on pCO_2 in the Greenland Sea was not predictable by SST, and *Cosca et al.* [2003] found that they could greatly improve their prediction of pCO_2 in the equatorial Pacific if biological indicators were included. These observations are particularly important when considering coastal seas, because biological activity and other biogeochemical reactions that modify pCO_2 independently of SST occur at disproportionately high rates in such areas [*Gattuso et al.*, 1998; *Wollast*, 1998]. To circumvent this problem, some researchers have attempted to include satellite-derived observations of ocean color in both the open ocean and coastal seas. *Ono et al.* [2004] were among the first to try this approach by using chlorophyll (Chl *a*) derived from an early ocean color sensor in a multivariate regression with SST. In a similar study, *Rangama* [2005] used Chl *a* derived from Sea-viewing Wide Field-of-view Sensor (SeaWiFS) to estimate pCO_2 in a region of the Southern Ocean.

The primary productivity in the upper ocean is also a key factor associated with the surface pCO_2 [*Ono et al.*, 2004; *Lohrenz and Cai*, 2006]. Therefore, there is the potential to remotely sense the surface pCO_2 using satellite data based on its correlation with SST, Chl *a*, and other key parameters. This has resulted in the development of empirical algorithms for satellite-derived pCO_2. Various algorithms have been derived for different areas of different spatial scales. In the North Pacific, *Stephens et al.* [1995] attempted to study the distribution of pCO_2 using remote sensing SST data. *Ono et al.* [2004] then introduced Chl *a* as an additional regression parameter and obtained reduced root-mean-square error (RMSE) when calculating pCO_2. *Sarma et al.* [2006] further developed a remote sensing algorithm for pCO_2, which contained three parameters, i.e., SST, Chl *a*, and climatological salinity (*S*). [*Lohrenz and Cai*, 2006] added colored dissolved organic matter (CDOM) as a parameter in their remote sensing algorithm for pCO_2, based on the good correlation existing between CDOM and *S* in the Mississippi plume.

The Baltic Sea is a semienclosed sea in Northern Europe characterized by restricted water exchange with the open ocean and a large inflow of river water [*Meier et al.*, 2014]. The pCO_2 displays considerable seasonal and interannual variability in the Baltic Sea and is affected by several processes, such as air-sea gas exchange, physical mixing, and various biological processes. Previous investigations of the Baltic Proper found large temporal and spatial variability in pCO_2. The amplitude of the annual pCO_2 cycle varies significantly depending on the region, ranging from 400 μatm in the northeastern Baltic Proper to 120 μatm in the transition areas to the North Sea [*Schneider and Kaitala*, 2006]. The Baltic Sea has been well studied [e.g., *Omstedt et al.*, 2004; *Hjalmarsson et al.*, 2008; *Backer and Leppänen*, 2008; *Wesslander*, 2011] and relatively well monitored and is well suited to the application of new methods for monitoring coastal seas that take account of river runoff [*Bergstrom*, 1994] and the importance of upwelling variability [*Myrberg and Andrejev*, 2003; *Lehmann and Myrberg*, 2008; *Norman et al.*, 2013]. The biogeochemical processes in the Baltic Sea marine environment are controlled mainly by the biological production and decomposition of organic matter occurring in the context of the regions hydrography [*Siegel and Gerth*, 2012]. Physical forcing controls the water transport, stratification, temperature, and *S* in the Baltic Sea; these factors then influence the nutrient and carbon distribution, thereby affecting biogeochemical processes. Monitoring the marine pCO_2 distribution on monthly to interannual timescales is therefore crucial to better understanding the carbon cycle [*Wesslander*, 2011]. Due to technical as well as financial limitations, in situ measurements of marine pCO_2 are sparse in space and time.

Parard et al. [2014] used the self-organizing multiple linear output (SOMLO) [*Sasse et al.*, 2013] method to estimate the ocean surface pCO_2 in the Baltic Sea from the remotely sensed SST, Chl *a*, CDOM, net primary production (NPP), and mixed-layer depth (MLD). The outputs of this research have a horizontal resolution of 4 km and cover the 1998–2011 period. We continue the work of *Parard et al.* [2014] by estimating pCO_2 variability in time and space over the Baltic Sea.

The manuscript is structured in five sections. After this introduction, section 2 presents the data and method used in this work. Section 3 presents the results divided into four subsections: section 3.1 examines the variability of pCO_2 estimated using the SOMLO method, section 3.2 examines the effect of variation in parameter forcing, section 3.3 examines coastal region variability, and section 3.4 estimates the climatology of pCO_2 for the year 2010. We conclude the article by discussing the results obtained.

2. Data and Method

2.1. pCO_2 Map

To reconstruct the sea surface pCO_2 concentrations, we employed the SOMLO methodology [*Sasse et al.*, 2013] in a similar way to that applied by *Parard et al.* [2014]. The SOMLO methodology combines two statistical approaches: *self-organizing maps* (SOMs) [*Kohonen*, 1990] and *linear regression*.

SOMs are a subfamily of neural network algorithms used to perform multidimensional classification. A defining characteristic of SOMs is that their classes can represent a Gaussian distribution centered on the typical profile of environmental parameters, if the training data set is highly discrete [*Dreyfus*, 2005]. During the training phase, the SOMLO methodology uses SOMs to discretize a data set of explanatory parameters in classes and then locally learn a set of linear regression coefficients to infer the pCO_2 for each class. When presented with a new vector of explanatory parameters, the methodology first classifies it on the SOM map and then uses the calculated regression coefficients to estimate the pCO_2.

In this paper, we introduce three major improvements in the methodology compared with that used in the previous study [*Parard et al.*, 2014]: (1) we divide the Baltic Basin into four sectors, applying SOMLO separately in each one; (2) we modify the classification process to take into account the covariance between parameters; and (3) we determine the regression coefficients over the principal component analysis projections of the data.

2.1.1. Division in Sectors

While the explanatory parameters considered (i.e., SST, Chl *a*, CDOM, NPP, and MLD) and information on the time of year (sine and cosine) have remained constant, compared with *Parard et al.* [2014], we had three sources of pCO_2 data which give 1445 vectors: the Östergarnsholm site with pCO_2 measurements from 2005 to 2011 [*Rutgersson et al.*, 2008] ; Cargo ship: this data set derives from continuous measurements of the surface water pCO_2 made in the Baltic Sea [*Schneider and Kaitala*, 2006; *Schneider et al.*, 2009]; Swedish Meteorological and Hydrological Institute database Svenskt Havsarkiv: pH and total alkalinity (TA) (http://www.smhi.se/klimatdata/oceanografi/havsmiljodata/marina-miljoovervakningsdata).

We added pCO_2 data to the pool of potential training data from vessel measurements, 2008–2010, in the Gulf of Bothnia shown in *Löffler et al.* [2012] (Figure 1) (B. Schneider, personal communication, 2014). In total, our data set now contains 1670 vectors compared with *Parard et al.* [2014]. It is all the data shown in the Gulf of Bothnia in Figure 1. The data can also be found in the Surface Ocean CO_2 Atlas ([*Bakker et al.*, 2014], SOCAT: www.socat.info). To optimize the SOM map size for the method and to calculate the method's performance, we randomly sampled 90% of the complete data set for use in the training phase, keeping 10% for use in computing the performance of the method.

The satellite data source is briefly presented here:

1. Sea surface temperature (SST): For 1998–2004 this data set consists of the monthly average SST (in °C) over the zone, with a spatial resolution of 4 km, extracted from version 5.2 of the advanced very high resolution radiometer (AVHRR) Pathfinder project [*Casey et al.*, 2010] (http://www.nodc.noaa.gov/SatelliteData/pathfinder4km/). For 2005–2011, we use data from the Federal Maritime and Hydrographic Agency, which processed data from AVHRR-NOAA, and data from the Group for High-Resolution Sea Surface Temperature data set for the Baltic Sea, 2007–2011. (http://podaac.jpl.nasa.gov/dataset/DMI-L4UHfnd-NSEABALTIC-DMI_OI).

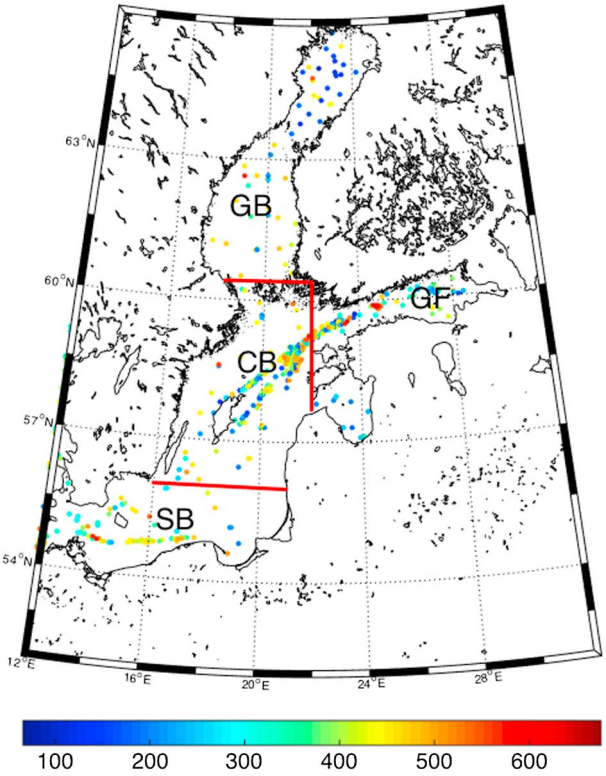

Figure 1. The location and quantity of available data in the Baltic Sea, 1998–2011. The color bar shows the pCO_2 value in µatm. The red lines indicate the division of the Baltic Basin into the Central Basin (CB), Gulf of Finland (GF), Gulf of Bothnia (GB), and South Basin (SB).

2. Chlorophyll *a* (Chl): for 1998–2011, from Sea-viewing Wide Field-of-view Sensor (SeaWiFS) with 4 km spatial and monthly temporal resolutions and Moderate Resolution Imaging Spectroradiometer (MODIS-Aqua) [*Casey et al.*, 2010].
3. Colored Dissolved Organic Matter (CDOM): the values come from MODIS-Aqua 4 km monthly average data *Morel and Gentili* [2009].
4. Net primary production (NPP): for 1998–2009 the Environmental Marine Information System [*Lee et al.*, 2005] and for 2009–2011 uses the Vertically Generalized Production Model of *Behrenfeld and Boss* [2006].
5. Mixed-layer dept (MLD): monthly averages from 1998 to 2007 *Burchard and Bolding* [2002] and for 2008–2011 [*Behrenfeld et al.*, 2005].

The details of theses different products are presented in *Parard et al.* [2014].

On studying the new data, we noticed that different geographic regions could present similar input vectors for the chosen explanatory parameters yet present vastly different pCO_2 concentrations. This suggested that different local process were driving the pCO_2 concentrations in each zone. Since these processes were not reflected by the selected parameters, we chose to separate the data in zones and apply the method in each data set.

Based on preexisting geographic separations, we chose to divide the Baltic Basin into four sectors: the Gulf of Bothnia, Gulf of Finland, Central Basin, and South Basin (Figure 1). The longitudinal and latitudinal limits of these regions are presented in Table 1.

We then trained the SOMLO methodology on the data belonging to each of these basins, reconstructing each point using each of the four SOMs. The final pCO_2 value for each point was then calculated by adding each of the four reconstructions weighted by a coefficient, w_i, inversely proportional to the square of the distance from the point being reconstructed to the center of each zone. More specifically,

$$\mathrm{Final}_{pCO_2}(x,y) = \sum_{i=1}^{4} w_i(x,y) \times pCO_2(i) \quad (1)$$

Table 1. The Four Basins Boundaries

Name of Basin	Latitude	Longitude
Gulf of Bothnia (GB)	≥ 60.4 °N	16°W ≤ longitude ≤ 26°W
Gulf of Finland (GF)	57°N < latitude ≤ 62°N	≥22°W
Central Basin (CB)	56°N ≤ latitude ≤ 60.4°N	13°W ≤ longitude ≤ 22°W
South Basin (SB)	≤56°N	All

$$w_i(x,y) = \frac{\frac{1}{\text{distance}([x,y],[\bar{x}_i,\bar{y}_i])}}{\sum_{i=1:4}\frac{1}{\text{distance}([x,y],[\bar{x}_i,\bar{y}_i])}} \tag{2}$$

where pCO_2(i) is the pCO_2 reconstructed using SOMLO trained over the data for each region and $\bar{x}_i$, $\bar{y}_i$ are the coordinates of the center of each region. This smoothing is essential to preserving the continuity between the four regions.

2.1.2. Modified Best Matching Unit

The selection of the best matching class is a particularly important part of the classification process. We introduced a change to the way we select the best matching class in order to favor local data correlations. When comparing an observation with each class of the topological map, the usual approach is to compare the observation (normalized in the same way as the training data sets) with the values of the referent vector of each class. The referent vector of each class corresponds is a vector containing the average values of the elements belonging to that class. If we represent a normalized observation by obs = (o_1, …, o_k), where k corresponds to the number of parameters classified in the SOM (minus one, i.e., the pCO_2) and the referent vector of class i by $r^i = (r^i_1, \ldots, r^i_k)$, then the best matching class is found by

$$\text{BMC}(\text{obs}, \text{SOM}) = \text{arg}_{\min_i} \sum_{i=k}^{n} \left(\sqrt{\sum_{j=1}^{k}(r^i_j - o_j)}\right) \tag{3}$$

where n corresponds to the number of classes in the SOM.

However, when trying to reconstruct the pCO_2 from other explanatory variables, we must take into account that the classes were generated using vectors containing the pCO_2. Each class represents a different dynamic of the system, in which the explanatory parameters are connected to the pCO_2 in different ways.

For each class we therefore calculated the absolute value of the covariances of the various parameters with pCO_2 and used this information to weigh our selection of the best matching class.

If we note $pCO^i_{2\text{cov}}$, i.e., the vector containing the absolute value of the covariance of each parameter of the elements captured by the ith neuron of the SOM with pCO_2, then the modified way to calculate the BMC is

$$\text{BMC}(\text{obs}, \text{SOM}) = \text{arg}_{\min_i} \sum_{i=1}^{n} \left(\sqrt{\sum_{j=1}^{k}((r^i_j - o_j) * (1 + pCO^i_{2\text{cov}}))^2}\right) \tag{4}$$

This version of the attribution to a class has the benefit of more effectively taking into account the covariance of the variables with the pCO_2, allowing certain extreme parameter values to be more easily associated with the areas of the SOM where the pCO_2 is more correlated with these values.

2.1.3. Regression Coefficients

The regression coefficients of the linear regression component of the SOMLO method were trained, as in *Parard et al.* [2014], on the data vectors belonging to the neighborhood of each class. We therefore had one set of linear regression coefficients per class for each map. Instead of including all the explanatory parameters, we chose to perform a principal component analysis [*Jolliffe*, 2002] of each of these training data sets. We chose to keep the first four axes of the principal component analysis and learn the regression coefficients for the data projections on these four axes. Before performing a reconstruction using the SOMLO method, we now project the explanatory parameters onto the axes of the classes to which they have been attributed and perform the regression on the scores thus obtained. This projection was used to obtain the pCO_2 based on

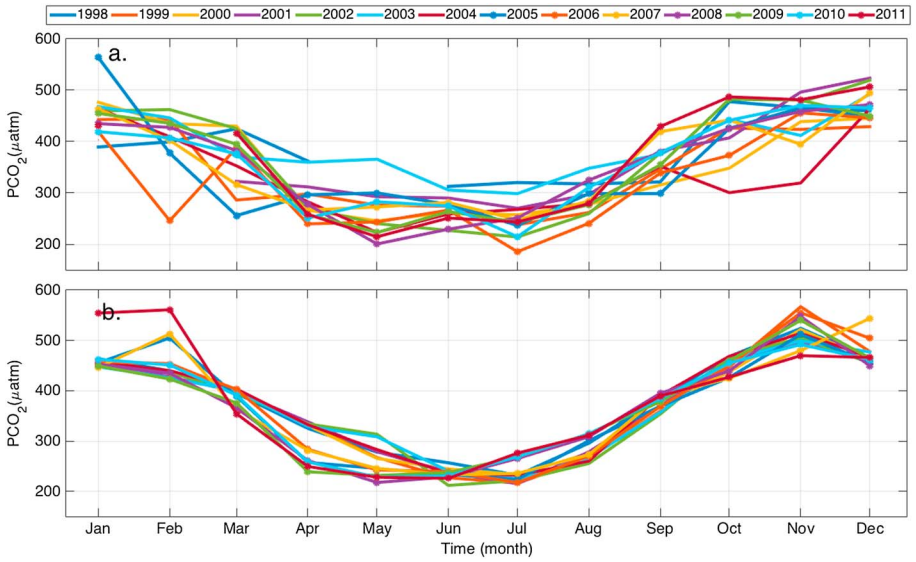

Figure 2. Annual pCO_2 cycle (a) Monthly average of the in situ data and (b) computed based on the satellite data for each interpolated year.

the most dominant parameters in each situation, discarding the axes describing a part of the variance that is less impactful.

3. Results

3.1. pCO_2 Map Description: Variability of pCO_2

The average in situ data for the 13 years from 1998 to 2011 are shown in Figure 2a. The SOMLO method [*Parard et al.*, 2014] allows the estimation of monthly pCO_2 maps for the entire Baltic Sea for the 13 years from 1998 to 2011, as shown in Figure 2b. As shown in Figure 1, the Baltic Sea is divided into four regions, i.e., the Gulf of Bothnia (GB), Gulf of Finland (GF), Central Basin (CB), and Southern Basin (SB). For the reconstructed pCO_2 values, the RMS values are lower and the correlation coefficients (R) are higher than those found in the previous study [*Parard et al.*, 2014]. The pCO_2 is well reproduced in each region (Table 2). The R values are good, the lowest being observed in the Southern Basin (0.9) where the RMS is the highest (i.e., 38.5 µatm). The Gulf of Finland has the highest R value (i.e., 0.97) and the Gulf of Bothnia the lowest RMS (19.5 µatm), the latter being the region with the lowest data density.

In Figure 2a, which shows the average pCO_2 values for each year, the seasonal variation is well reproduced with lower values in summer and higher values in winter. The variability of the in situ data has the same order of magnitude than the computed pCO_2 with SOMLO method (Figure 2).

The atmospheric pCO_2 was estimated using the method from *Rutgersson et al.* [2009]. From April to about October, the pCO_2 is clearly below the atmospheric pCO_2, which was 362–404 µatm from 1997 to 2011 (Figures 3 and 4). *Omstedt et al.* [2014] attributed the low pCO_2 values to CO_2 consumption by biological processes that control pCO_2 from April to October dominating the effect of rising temperatures in spring and summer that would increase pCO_2. The seasonal pCO_2 distribution is characterized by the two minima observed in spring and midsummer (Figures 3 and 4), resulting from interplay between production peaks and

Table 2. RMS Values and Correlation Coefficients for the Reconstructed pCO_2 Values

Region	R	RMS (µatm)
Gulf of Bothnia	0.97	19.5
Gulf of Finland	0.98	25.8
Central Basin	0.96	34.0
South Basin	0.90	38.5

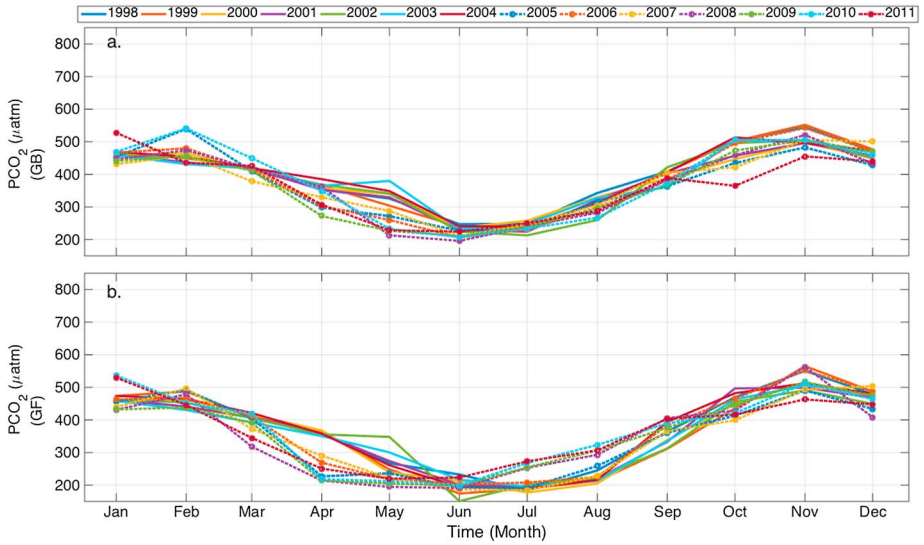

Figure 3. Variability of mean pCO_2 in (a) the Gulf of Bothnia and (b) the Gulf of Finland.

increasing temperatures [*Omstedt et al.*, 2014]. The pCO_2 increase after the main productive period coincides with the deepening of the mixed-layer transporting CO_2-enriched water masses to the surface. This process causes oversaturation of the surface water relative to atmospheric CO_2, so CO_2 is released into the atmosphere from November to March. This is coherent with the satellite data distribution of the input parameters, the mixed-layer depth (MLD) being deeper and SST being higher in the spring (Figure 5a). Chl *a* is higher in spring and summer (Figure 5b), and NPP is high in spring (Figure 6a), corresponding to the period of the first high biological activity.

The mean pCO_2 values are computed for each of those four basins defined separately (Figures 3 and 4), i.e., the Gulf of Bothnia (GB), Gulf of Finland (GF), Central Basin (CB), and Southern Basin (SB) (Figure 1). The variability is similar in all four basins, but the increase in summer is higher in the Gulf of Finland than in the other basins (Figure 3b) and lower in the South basin (SB) than in the other basins (Figure 4b). The interannual variability is lower in the Central Basin than in the other basins. The decrease in mean pCO_2 observed in Figure 2b in May from 2007 to 2011 is due to variability in the gulfs of Finland and Bothnia. The pCO_2 variability is higher in the gulfs of Finland and Bothnia, with standard deviations of 11.4 and 17.6 µatm, respectively, compared with those of the South and Central Basins of 8.9 and 6.4 µatm, respectively. The Gulf of Finland and Central

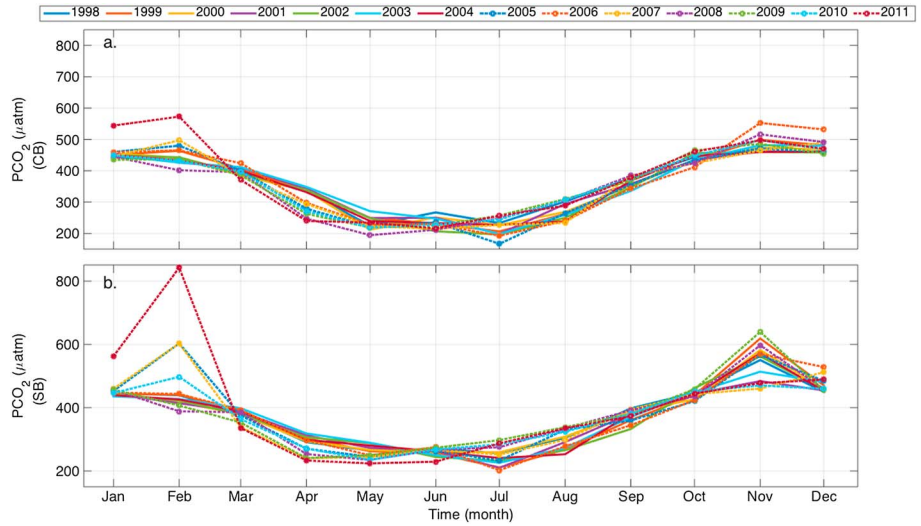

Figure 4. Variability of mean pCO_2 in (a) the Central Basin and (b) the South Basin.

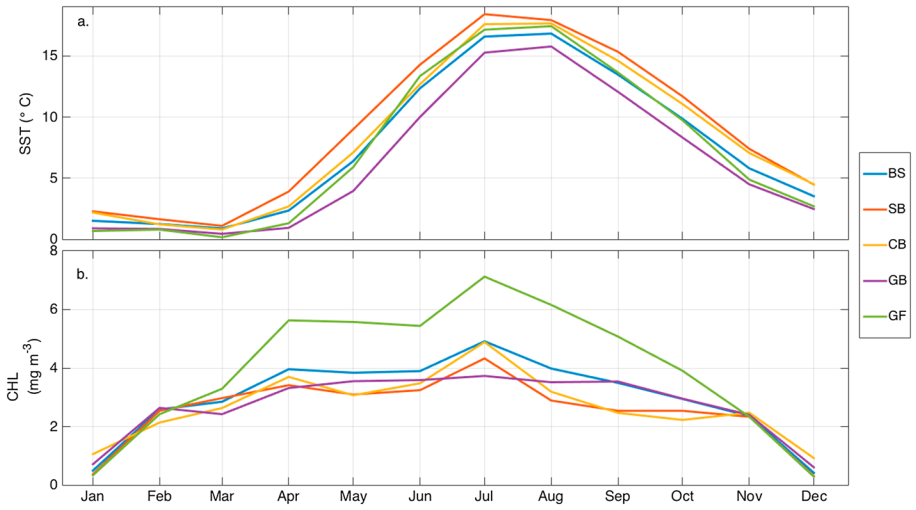

Figure 5. Evolution of average parameter values in each basin (the entire Baltic Sea (BS), South Basin (SB), Central Basin (CB), Gulf of Bothnia (GB), and Gulf of Finland (GF)) for (a) SST and (b) Chl *a*.

Basin have nearly the same values with averages of 350.6 and 350.9 µatm, respectively, the South Basin being slightly higher with an average of 369.6 µatm and the Gulf of Bothnia the highest with a value of 384.4 µatm.

3.2. Variation in Forcing Parameters

All parameters used to compute the pCO_2 map can be used in estimating the important processes for the entire Baltic Sea and for each basin separately. Figures 5 and 6 show the monthly averages of all parameters. The evolution is fairly similar in all basins, but in the Gulf of Finland, the Chl *a* and NPP values are higher than in the other basins, though its SST and MLD values remain in same order of magnitude as in the other basins. CDOM, a parameter that cannot be removed when computing the pCO_2 [*Parard et al.*, 2014], has low variability. This low CDOM variability could be due to a lack of satellite data, so the effect of CDOM on pCO_2 is likely underestimated.

Strong interannual variability in pCO_2 is observed (Figure 2). The pCO_2 minimum is usually observed in June and July, but from 2007 to 2011 the minimum is observed in May (Figure 2). For 2005 and 2006, two minima are observed in May and July. SST, Chl *a*, MLD, CDOM, and NPP—parameters used to construct the pCO_2 map—all display interannual variability, the strongest being observed in MLD, Chl *a*, and NPP. The interannual variability in MLD is very strong in winter and early spring. Chl *a* is stronger after 2005, representing a positive

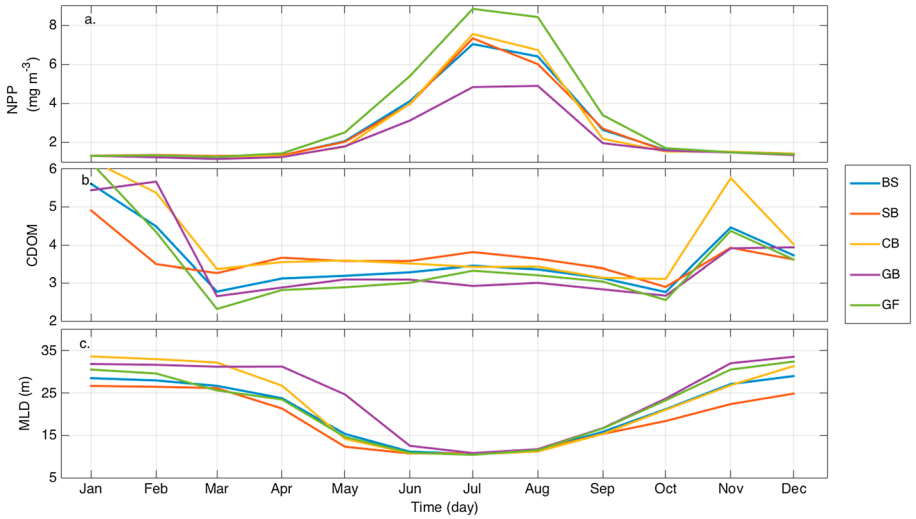

Figure 6. Evolution of average parameter values in each basin (the entire Baltic Sea (BS), South Basin (SB), Central Basin (CB), Gulf of Bothnia (GB), and Gulf of Finland (GF)) for (a) NPP, (b) CDOM, and (c) MLD.

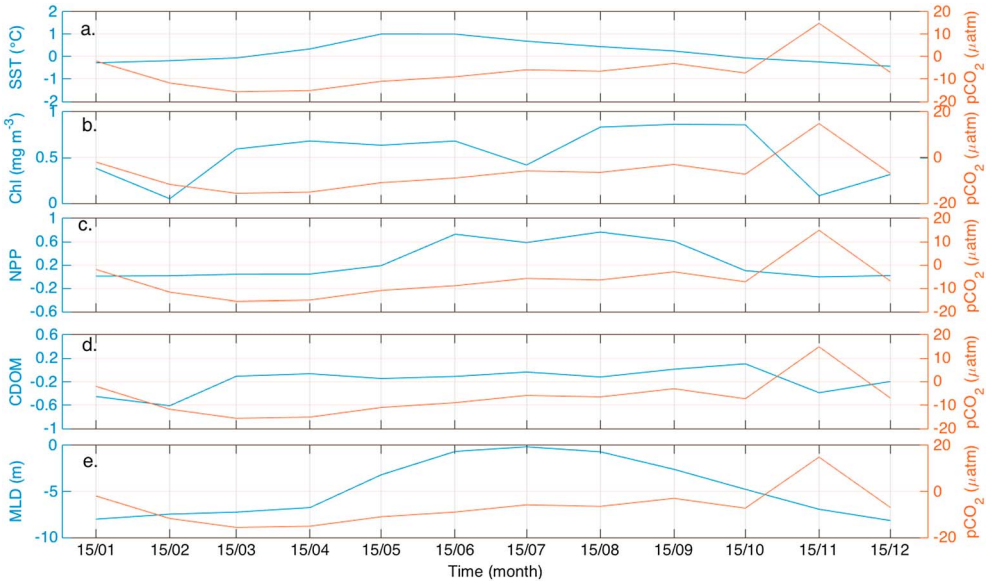

Figure 7. The difference between the coastal and open sea regions. The red scale on the right side is for the difference in pCO_2, and the blue scale on the left is for the difference in various other parameters: (a) SST, (b) Chl *a*, (c) NPP, (d) CDOM, and (e) MLD.

anomaly compared with the mean yearly Chl *a*, but before this the anomaly is negative. The NPP interannual variability occurs in spring and summer; the maximum observed NPP displays strong temporal variability, which influences the variability in the pCO_2 minimum observed during this period.

MLD is deeper in the Gulf of Bothnia than in the other basins, this deeper mixing explaining the higher pCO_2 value. The Gulf of Finland displays a lower pCO_2 value, while the difference in the Central Basin is approximately 20 μatm. The Chl *a* and NPP values are higher in the Central Basin in spring and summer, possibly because biological activity exerts a stronger effect than in the other basins.

MLD displays variability within each year. The highest variability is observed in the South and Central Basins, where MLD can differ by approximately 20 m in years such as 2008 and 2000. The SST and Chl *a* variability is of the same order of magnitude for each basin, indicating that these parameters are not majorly responsible for the observed differences. NPP displays strong variability between May and October in the Gulf of Finland, representing a positive anomaly compared with the average, so the NPP value is stronger year round than in the Gulf of Bothnia, where NPP is below average and where lower variability is also observed. No NPP trend is evident in the South and Central Basins, though NPP varies from approximately −5 to 5 mg m^{-3}. CDOM variability is stronger in the South Basin, possibly because more data are available for this area.

3.3. Coastal Variability

The pCO_2 map allows us to divide the pCO_2 and all other parameters between the coastal region and the open sea. The coastal region is defined by a distance of 0.5° in latitude and longitude from the coast; farther than this from the coast is defined as open sea.

Figure 7 shows that the mean pCO_2 difference between the coastal region and the open sea is negative (i.e., −10 μatm). Coastal pCO_2 values are lower than open sea values in the spring and early summer. On average, a greater difference in pCO_2 is observed between February and June, when it varies between 8 and 16 μatm. The pCO_2 difference between the coastal region and open sea is attributable to the difference in forcing parameters. In November, we observed a large difference between the coastal and open sea pCO_2, with a higher value in the coastal area (Figure 7). We observed the opposite signal in CDOM and Chl *a* compare to pCO_2 variability, with higher values in the open sea than along the coast. It is logical that the Chl *a* and CDOM values should be higher near the coast in winter, and this could explain the observed difference in pCO_2 between the coast and open sea.

The parameter signals differ between spring and midsummer. SST is 0.25–1°C warmer between April and September in the open sea than in the coastal region (Figure 7a). This causes an increase in pCO_2 due to

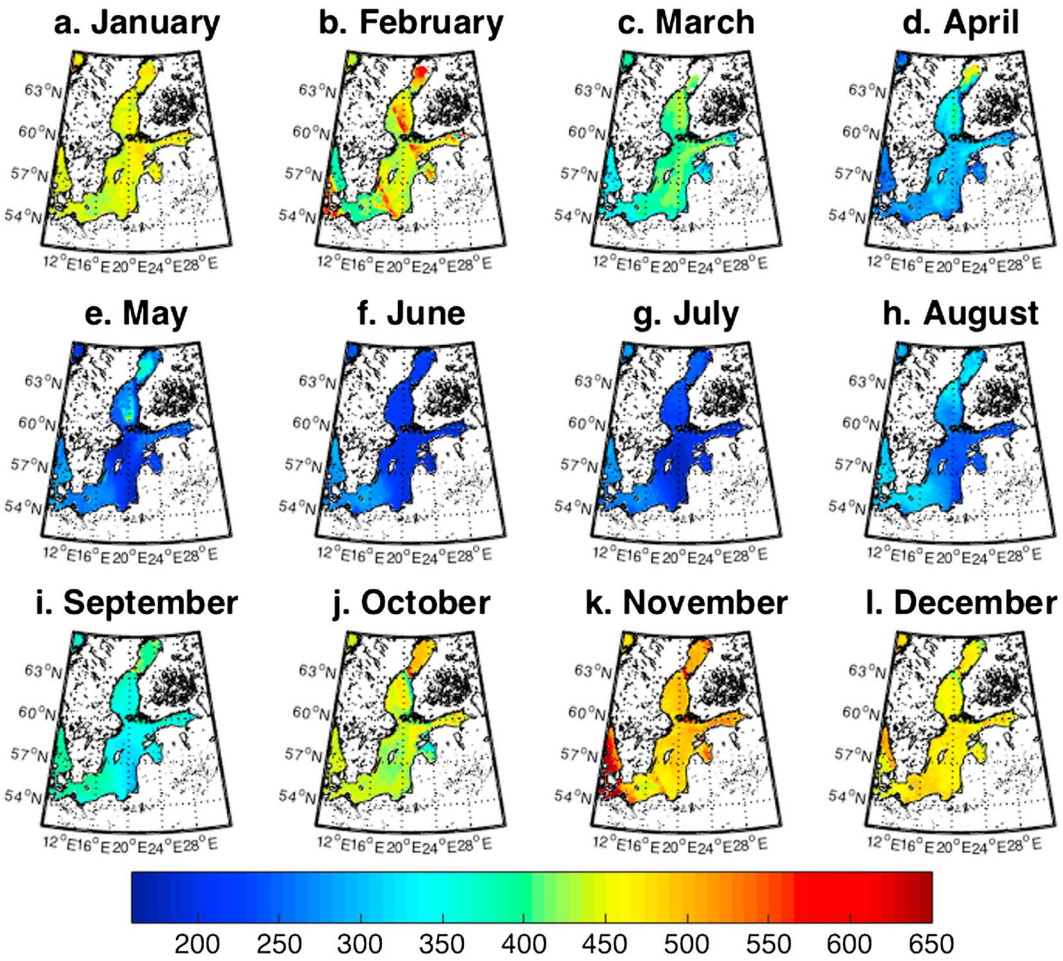

Figure 8. Monthly climatology of pCO_2 for the January–December period.

the thermodynamic effect, and the pCO_2 follows a slope of 4.23% (°C)$^{-1}$ [*Takahashi et al.*, 1993]. The pCO_2 in the coastal region is lower. Chl *a* is higher in the coastal region between March and October, averaging 0.7 mg m^{-3} with a variability range of 0.4–0.9 mg m^{-3}. NPP is also higher near the coast with an average of 0.4 and a variability range of 0.03–0.8 mg m^{-2} between March and October and a higher value between May and September when biological activity is stronger. Chl *a* and NPP are the parameters responsible for the variability in pCO_2 before April. The increase in Chl *a* and NPP near the coast can explain the lower pCO_2 value, attributable to biological consumption (Figures 7b and 7d). CDOM is lower, averaging 0.06 mg m^{-3} with a lower value between March and August. The within-year difference is very small, the greater difference being observed in the Gulf of Finland (0.59 mg m^{-3}) and the Central Basin (0.8 mg m^{-3}). In the Gulf of Finland, the coastal region CDOM is lower between May and August, while in the Central Basin it is lower in winter. CDOM absorption reduces the penetration of UV light into the water column, protecting marine organisms from exposure to harmful UV radiation while reducing the amount of visible light available for pelagic and benthic photosynthesis [*Bidigare et al.*, 1993]. CDOM increases with greater turbidity and lower *S* [*Bowers et al.*, 2004]. The average CDOM is slightly higher in the open sea than in the coastal region, but this cannot help to conclude about the difference in turbidity is not significant. MLD is always deeper in the open sea (Figure 7e), which must increase the pCO_2 in this region. The biological consumption is higher in the coastal region, while the higher MLD and higher SST explain the higher pCO_2 in the open sea region.

In the Baltic Sea, upwelling happens often [*Myrberg and Andrejev*, 2003] between June and September. The length scale is typically 75–100 km and the width scale 10–30 km, while the lifetime of the feature varies between 0.5 and 10 days and the temperature difference is typically 2–4°C. On a monthly scale, the upwelling signature is not visible in the satellite data, so we can study this effect in the coastal region only at higher temporal resolutions.

3.4. Climatology of pCO_2 in Baltic Sea

The climatology of pCO_2 is estimated from the pCO_2 map constructed from 1998 to 2011 (Figure 8), which permits the observation of both temporal and spatial variability. We can observe spatial variability, pCO_2 generally being higher in the north than the south, except in summer in the south where the value is higher than in the central part. Some parts of the north lack data due to ice cover in winter.

The number of data is limited, which limits the validity of the method, but the results are convincing compared with those of other similar studies of the Baltic Sea [e.g., *Friedrich and Oschlies*, 2009; *Hales et al.*, 2012; *Landschützer et al.*, 2013]. In the future, increasing the number of NPP and CDOM data could improve our estimates, while adding certain parameters, such as *S*, could permit better descriptions of the various processes operative in each region.

4. Discussion

It remains difficult to reliably assess variations in pCO_2 in the global oceans, including the marginal seas, due primarily to the lack of sufficient spatial and temporal pCO_2 field measurements in these complex regions [*Canadell*, 2003]. Remote sensing with applicable algorithms could certainly be an important approach complementing shipboard observations. Using this method, we provide the first estimate of pCO_2 climatology in the Baltic Sea based on satellite data. The mean pCO_2 is 368.3 $\pm$ 100 µatm, with a range of 234–514 µatm. The seasonal variability in pCO_2 is strong, with the lowest pCO_2 observed in summer (i.e., 282 µatm) and the highest pCO_2 observed in winter (i.e., 469 µatm). The higher value was observed in 1998, accompanied by low variability of 97 µatm, and the lower value was observed in 2011, accompanied by higher variability (121 µatm); however, the lowest variability (i.e., 95.7 µatm) was observed in 2003. The variability was strong between 2009 and 2011, with higher variability observed in the North and East Basins. NPP and MLD are the parameters having the strongest influence on the basin variability in pCO_2 and are also parameters displaying strong interannual variability.

Furthermore, separating the Baltic Basin into four regions improves the results of estimating the pCO_2, lowering the RMS (<40 µatm) and increasing the correlation coefficient ($R > 0.96$). One possible reason for the difference in parameter variability between the regions is the variability in *S*. The Baltic Sea is characterized by its large differences in *S*. From approximately 25 ppm in the Kattegat, it decreases to 8 ppm in the southern Baltic Sea and to only 2 ppm in the northern Gulf of Bothnia and the innermost Gulf of Finland [*Feistel et al.*, 2010].

Beldowski et al. [2010] demonstrate that total CO_2 is controlled mainly by alkalinity (AT) and by the production and decomposition of organic matter. In oceanic surface water, changes in AT are caused mainly by evaporation and precipitation and the AT/*S* ratio is almost constant [*Lee et al.*, 2006]. The situation differs in the Baltic Sea [*Wesslander*, 2011], where the surface water AT is controlled by the mixing of oceanic water originating from the North Atlantic with river water containing varying amounts of AT. It was proven that surface AT distributions are controlled largely by the spatially varying riverine AT input and by mixing with the ocean water that enters the Baltic Sea via the Kattegat. This is in agreement with some studies demonstrating that taking account of *S* in the North Atlantic Ocean improves the estimation of pCO_2 using a method similar to ours [*Nakaoka et al.*, 2013]. *Thomas and Schneider* [1999] observed correlation between the associated changes in dissolved inorganic carbon (DIC) and *S* between summer and winter. Corresponding to the increase in the seasonal changes in *S*, the changes in DIC increase. In the future, adding a parameter such as *S* to the vector would improve the method, allowing the use of one map for the entire basin rather than one divided into four basins.

In the present study, NPP and MLD are important parameters when estimating the pCO_2. As biological activity is very important in summer, these parameters are more important in the coastal area than in the open ocean, as explained by *Chierici et al.* [2009]. Taking account of in situ CDOM measurement improved our results, but since the quality of the satellite CDOM measurements may be too imprecise when compared to the in situ measurements, we chose to exclude them. The Chl *a* gives us information on the biological activity on a monthly timescale, but the bloom takes place at a lower scale so we lost the information. It will be really interesting to improve this work on a shorter temporal scale to work on processes like the coastal upwelling. Several other studies have used a similar neural method, most of them using SST and Chl *a* and sometimes MLD. One study [*Chang et al.*, 2013] estimated net community production using several data products:

photosynthetically available radiation, particulate organic carbon, Chl *a*, SST, sea surface height, and MLD (from dioxygen argon measurements). The nonlinearity of these methods present, however, the disadvantage of not being able to provide a robust uncertainty estimation such as those provided in more linear approaches [i.e., *Omar et al.*, 2007]. We are therefore making the hypothesis that the errors in the predictors are such that they still get classified in the correct class of the SOM. We plan on further exploring the uncertainty analysis of such methods in future papers.

In comparison, existing studies performed over the North Atlantic and North Pacific are based on a minimum of 10,000 data points (which take into account all the data from SOCAT) to a maximum of 800,000 data points [e.g., *Telszewski et al.*, 2009; *Friedrich and Oschlies*, 2009; *Hales et al.*, 2012; *Landschützer et al.*, 2013]. In North Atlantic, *Friedrich and Oschlies* [2009] obtained an RMS error (RMSE) of 19 µatm for the year 2005. A similar study over the entire Atlantic Ocean obtained an RMSE of 17 µatm for independent time series [*Landschützer et al.*, 2013]. *Hales et al.* [2012] obtained an RMSE of 20 µatm with a correlation coefficient of 0.81. The RMSE obtained here was higher than that obtained in a previous study of the Atlantic Ocean, but, taking into account the much smaller number of data available and the possibly stronger spatial pCO_2 variability in the Baltic Sea than the open ocean, the results presented here are promising. Another study in the northern South China Sea [*Jo et al.*, 2012] applied a neural network method with four inputs (SST, Chl *a*, longitude, and latitude). Their results revealed a high correlation coefficient of 0.98 with a root-mean-square error (RMSE) of 6.9 µatm. However, their model is trained and applied on a relatively small coastal area with less variability than the one present in the Baltic Sea.

Acknowledgments

The authors would like to thank Tiit Kutser and Melissa Chierici for their valuable help with data collection. We would like to thank Sylvie Thiria for advice on the SOM classifications and Marion Leduc-Leballeur for help with the method for filling the gaps in satellite data. We would also like to thank Bernd Schneider and the BONUS/Baltic-C programs for Cargo Ship Observations. The satellite data used for the pCO_2 estimations are available at http://www.nodc.noaa.gov/SatelliteData/pathfinder4km/ for SST, http://oceandata.sci.gsfc.nasa.gov for CDOM and NPP (2008–2011), www.getm.eu for NPP, and http://emis.jrc.ec.europa.eu for MLD and Chl *a*. The pCO_2 estimation will be available at http://www.geo.uu.se/forskning/luval/amnen//meteorologi/pagaende-forskning/vatten-och-atmosfar/ web page. We would like to thank the Swedish National Space Board (120/11:3) for financing the project.

References

Backer, H., and J.-M. Leppänen (2008), The HELCOM system of a vision, strategic goals and ecological objectives: Implementing an ecosystem approach to the management of human activities in the Baltic Sea, *Aquatic Conserv: Mar. Freshw. Ecosyst.*, *18*(3), 321–334.

Bakker, D. C. E., et al. (2014), An update to the Surface Ocean CO2 Atlas (SOCAT version 2), *Earth Syst. Sci. Data*, *6*, 69–90, doi:10.5194/essd-6-69-2014.

Behrenfeld, M. J., and E. Boss (2006), Beam attenuation and chlorophyll concentration as alternative optical indices of phytoplankton biomass, *J. Mar. Res.*, *64*(3), 431–451.

Behrenfeld, M. J., E. Boss, D. A. Siegel, and D. M. Shea (2005), Carbon-based ocean productivity and phytoplankton physiology from space, *Global Biogeochem. Cycles*, *19*, GB1006, doi:10.1029/2004GB002299.

Beldowski, J., A. Löffler, B. Schneider, and L. Joensuu (2010), Distribution and biogeochemical control of total CO_2 and total alkalinity in the Baltic Sea, *J. Mar. Syst.*, *81*(3), 252–259.

Bergstrom, S. (1994), River runoff to the Baltic Sea: 1950–1990, *Ambio*, *23*, 280–287.

Bidigare, R. R., M. E. Ondrusek, and J. M. Brooks (1993), Influence of the Orinoco River outflow on distributions of algal pigments in the Caribbean Sea, *J. Geophys. Res.*, *98*(C2), 2259–2269.

Borges, A. V. (2011), Present day carbon dioxide fluxes in the coastal ocean and possible feedbacks under global change, in *Oceans and the Atmospheric Carbon Content*, edited by P. M. da Silva Duarte and J. M. Santana-Casiano, pp. 47–77, Springer, Netherlands.

Borges, A. V., B. Delille, and M. Frankignoulle (2005), Budgeting sinks and sources of CO_2 in the coastal ocean: Diversity of ecosystems counts, *Geophys. Res. Lett.*, *32*, L14601, doi:10.1029/2005GL023053.

Bowers, D. G., D. Evans, D. N. Thomas, K. Ellis, and P. J. I. B. Williams (2004), Interpreting the colour of an estuary, *Estuarine Coastal Shelf Sci.*, *59*(1), 13–20.

Burchard, H., and K. Bolding (2002), GETM: A General Estuarine Transport Model. Scientific documentation, *Rep. EUR 20253*, Eur. Comm., Joint Res. Cent., Inst. for Environ. and Sustainability, Ispra Italy.

Canadell, J. G. (2003), *Global Carbon Project: The Science Framework and Implementation*, Global Carbon Project, Canberra.

Casey, K. S., T. B. Brandon, P. Cornillon, and R. Evans (2010), The past, present, and future of the AVHRR Pathfinder SST program, in *Oceanography From Space*, edited by V. Barale, J. F. R. Gower, and L. Alberotanza, pp. 273–287, Springer, Netherlands.

Chang, C.-H., N. C. Johnson, and N. Cassar (2013), Neural network-based estimates of southern ocean net community production from in-situ O_2/Ar and satellite observation: A methodological study, *Biogeosci. Discuss.*, *10*, 16,923–16,972.

Chierici, M., A. Olsen, T. Johannessen, J. Trinañes, and R. Wanninkhof (2009), Algorithms to estimate the carbon dioxide uptake in the northern North Atlantic using shipboard observations, satellite and ocean analysis data, *Deep Sea Res., Part II*, *56*(8), 630–639.

Cosca, C. E., R. A. Feely, J. Boutin, J. Etcheto, M. J. McPhaden, F. P. Chavez, and P. G. Strutton (2003), "Seasonal and interannual CO_2 fluxes for the central and eastern equatorial Pacific Ocean as determined from f CO_2-SST relationships", *J. Geophys. Res.*, *108*(C8), 3278, doi:10.1029/2000JC000677.

Dreyfus, G. (2005), *Neural Networks: Methodology and Applications*, Springer, Berlin and New York.

Feistel, R., S. Weinreben, H. Wolf, S. Seitz, P. Spitzer, B. Adel, G. Nausch, B. Schneider, and D. G. Wright (2010), Density and absolute salinity of the Baltic Sea 2006–2009, *Ocean Sci.*, *6*(1), 3–24.

Frankignoulle, M., and A. V. Borges (2001), European continental shelf as a significant sink for atmospheric carbon dioxide, *Global Biogeochem. Cycles*, *15*(3), 569–576.

Friedrich, T., and A. Oschlies (2009), Neural network-based estimates of north Atlantic surface pCO_2 from satellite data: A methodological study, *J. Geophys. Res.*, *114*, C03020, doi:10.1029/2007JC004646.

Gattuso, J.-P., M. Frankignoulle, and R. Wollast (1998), Carbon and carbonate metabolism in coastal aquatic ecosystems, *Annu. Rev. Ecol. Syst.*, *29*, 405–434.

Hales, B., P. G. Strutton, M. Saraceno, R. Letelier, T. Takahashi, R. Feely, C. Sabine, and F. Chavez (2012), Satellite-based prediction of pCO_2 in coastal waters of the eastern North Pacific, *Prog. Oceanogr.*, *103*, 1–15, doi:10.1016/j.pocean.2012.03.001.

Hjalmarsson, S., K. Wesslander, L. G. Anderson, A. Omstedt, M. Perttilä, and L. Mintrop (2008), Distribution, long-term development and mass balance calculation of total alkalinity in the Baltic Sea, *Cont. Shelf Res.*, *28*(4), 593–601.

Hood, E. M., and L. Merlivat (2001), Annual to interannual variations of f CO_2 in the Northwestern Mediterranean Sea: High frequency time series data from CARIOCA buoys (1995–1997), *J. Mar. Res.*, *59*, 113–31.
Jamet, C., C. Moulin, and N. Lefèvre (2007), Estimation of the oceanic pCO_2 in the north Atlantic from VOS lines in-situ measurements: Parameters needed to generate seasonally mean maps, *Ann. Geophys.*, *25*, 2247–2257, Copernicus EGU.
Jo, Y.-H. . H., M. Dai, W. Zhai, X.-H. . H. Yan, and S. Shang (2012), On the variations of sea surface pCO_2 in the northern South China Sea: A remote sensing based neural network approach, *J. Geophys. Res.*, *117*, C08022, doi:10.1029/2011JC007745.
Jolliffe, I. T. (2002), *Principal Component Analysis*, Springer, New York.
Kohonen, T. (1990), The self-organizing map, *Proc. IEEE*, *78*(9), 1464–1480.
Landschützer, P., N. Gruber, D. C. E. Bakker, U. Schuster, S. Nakaoka, M. R. Payne, T. P. Sasse, and J. Zeng (2013), A neural network-based estimate of the seasonal to inter-annual variability of the Atlantic ocean carbon sink, *Biogeosciences*, *10*(11), 7793–7815.
Laruelle, G. G., R. Lauerwald, B. Pfeil, and P. Regnier (2014), Regionalized global budget of the CO_2 exchange at the air-water interface in continental shelf seas, *Global Biogeochem. Cycles*, *28*, 1199–1214, doi:10.1002/2014GB004832.
Lee, K., R. Wanninkhof, T. Takahashi, S. C. Doney, and R. A. Feely (1998), Low interannual variability in recent oceanic uptake of atmospheric carbon dioxide, *Nature*, *396*(6707), 155–159.
Lee, K., L. T. Tong, F. J. Millero, C. L. Sabine, A. G. Dickson, C. Goyet, G.-H. Park, R. Wanninkhof, R. A. Feely, and R. M. Key (2006), Global relationships of total alkalinity with salinity and temperature in surface waters of the world's oceans, *Geophys. Res. Lett.*, *33*, L19605, doi:10.1029/2006GL027207.
Lee, Z.-P., M. Darecki, K. L. Carder, C. O. Davis, D. Stramski, and W. J. Rhea (2005), Diffuse attenuation coefficient of downwelling irradiance: An evaluation of remote sensing methods, *J. Geophys. Res.*, *110*, C02017, doi:10.1029/2004JC002573.
Lefèvre, N., and A. Taylor (2002), Estimating pCO_2 from sea surface temperatures in the Atlantic gyres, *Deep Sea Res., Part I*, *49*(3), 539–554.
Lefévre, N., A. J. Watson, and A. R. Watson (2005), A comparison of multiple regression and neural network techniques for mapping in situ pCO_2 data, *Tellus B*, *57*(5), 375–384, doi:10.1111/j.1600-0889.2005.00164.x.
Lehmann, A., and K. Myrberg (2008), Upwelling in the Baltic Sea: A review, *J. Mar. Syst.*, *74*, S3–S12.
Löffler, A., B. Schneider, M. Perttilä, and G. Rehder (2012), Air–sea CO_2 exchange in the Gulf of Bothnia, Baltic Sea, *Cont. Shelf Res.*, *37*, 46–56.
Lohrenz, S. E., and W.-J. Cai (2006), Satellite ocean color assessment of air-sea fluxes of CO_2 in a river-dominated coastal margin, *Geophys. Res. Lett.*, *33*, L01601, doi:10.1029/2005GL023942.
Meier, H. E. M., A. Rutgersson, and M. Reckermann (2014), An Earth system science program for the Baltic Sea region, *Eos, Trans. AGU*, *95*(13), 109–110.
Morel, A., and B. Gentili (2009), A simple band ratio technique to quantify the colored dissolved and detrital organic material from ocean color remotely sensed data, *Remote Sens. Environ.*, *113*(5), 998–1011.
Myrberg, K., and O. Andrejev (2003), Main upwelling regions in the Baltic Sea—A statistical analysis based on three-dimensional modelling, *Boreal Environ. Res.*, *8*(2), 97–112.
Nakaoka, S., M. Telszewski, Y. Nojiri, S. Yasunaka, C. Miyazaki, H. Mukai, and N. Usui (2013), Estimating temporal and spatial variation of ocean surface pCO_2 in the north pacific using a self-organizing map neural network technique, *Biogeosciences*, *10*, 6093–6106.
Nelson, N. B., N. R. Bates, D. A. Siegel, and A. F. Michaels (2001), Spatial variability of the CO_2 sink in the Sargasso Sea, *Deep Sea Res., Part II*, *48*(8), 1801–1821.
Norman, M., S. Raj Parampil, A. Rutgersson, and E. Sahlée (2013), Influence of coastal upwelling on the air-sea gas exchange of CO_2 in a Baltic Sea basin, *Tellus B*, *65*, 21831.
Olsen, A., R. G. Bellerby, T. Johannessen, A. M. Omar, and I. Skjelvan (2003), Interannual variability in the wintertime air–sea flux of carbon dioxide in the northern North Atlantic, 1981–2001, *Deep Sea Res., Part I*, *50*(10), 1323–1338.
Olsen, A., J. A. Triñanes, and R. Wanninkhof (2004), Sea–air flux of CO_2 in the Caribbean sea estimated using in situ and remote sensing data, *Remote Sens. Environ.*, *89*(3), 309–325.
Omar, A. M., T. Johannessen, A. Olsen, S. Kaltin, and F. Rey (2007), Seasonal and interannual variability of the air–sea CO_2 flux in the Atlantic sector of the Barents Sea, *Mar. Chem.*, *104*(3), 203–213.
Omstedt, A., J. Elken, A. Lehmann, and J. Piechura (2004), Knowledge of the Baltic Sea physics gained during the BALTEX and related programmes, *Prog. Oceanogr.*, *63*(1), 1–28.
Omstedt, A., C. Humborg, J. Pempkowiak, M. Perttilä, A. Rutgersson, B. Schneider, and B. Smith (2014), Biogeochemical control of the coupled CO_2–O_2 system of the Baltic Sea: A review of the results of BALTIC-C, *Ambio*, *43*(1), 49–59.
Ono, T., T. Saino, N. Kurita, and K. Sasaki (2004), Basin-scale extrapolation of shipboard pCO_2 data by using satellite SST and chl a, *Int. J. Remote Sens.*, *25*(19), 3803–3815.
Parard, G., A. A. Charantonis, and A. Rutgerson (2014), Remote sensing algorithm for sea surface CO_2 in the Baltic Sea, *Biogeosci. Discuss.*, *11*, 12,255–12,294, doi:10.5194/bgd-11-12255-2014.
Rangama, Y. (2005), Variability of the net air–sea CO_2 flux inferred from shipboard and satellite measurements in the southern Ocean South of Tasmania and New Zealand, *J. Geophys. Res.*, *110*, C09005, doi:10.1029/2004JC002619.
Rutgersson, A., M. Norman, B. Schneider, H. Pettersson, and E. Sahlée (2008), The annual cycle of carbon dioxide and parameters influencing the air–sea carbon exchange in the Baltic Proper, *J. Mar. Syst.*, *74*(1), 381–394, doi:10.1016/j.jmarsys.2008.02.005.
Rutgersson, A., M. Norman, and G. Aström (2009), Atmospheric CO_2 variation over the Baltic Sea and the impact on air-sea exchange, *Boreal Environ. Res.*, *14*(1), 238–249.
Sarma, V., T. Saino, K. Sasaoka, Y. Nojiri, T. Ono, M. Ishii, H. Y. Inoue, and K. Matsumoto (2006), Basin-scale pCO_2 distribution using satellite sea surface temperature, chl a, and climatological salinity in the North Pacific in spring and summer, *Global Biogeochem. Cycles*, *20*, GB3005, doi:10.1029/2005GB002594.
Sasse, T. P., B. I. McNeil, and G. Abramowitz (2013), A novel method for diagnosing seasonal to inter-annual surface ocean carbon dynamics from bottle data using neural networks, *Biogeosciences*, *10*, 4319–4340.
Schneider, B., and S. Kaitala (2006), Identification and quantification of plankton bloom events in the Baltic Sea by continuous pCO_2 and chlorophyll a measurements on a cargo ship, *J. Mar. Syst.*, *59*, 238–248.
Schneider, B., S. Kaitala, M. Raateoja, and B. Sadkowiak (2009), A nitrogen fixation estimate for the Baltic Sea based on continuous pCO_2 measurements on a cargo ship and total nitrogen data, *Cont. Shelf Res.*, *29*(11), 1535–1540, doi:10.1016/j.csr.2009.04.001.
Schuster, U., et al. (2013), An assessment of the Atlantic and Arctic sea-air CO_2 fluxes, 1990-2009, *Biogeosciences*, *10*, 607–627.
Siegel, H., and M. Gerth (2012), Baltic Sea environment fact sheet sea surface temperature in the Baltic Sea in 2011, HELCOM Baltic Sea Environment Fact Sheets [online]. [Available at http://www.helcom.fi/baltic-sea-trends/ environment-fact-sheets/.]
Stephens, M. P., G. Samuels, D. B. Olson, R. A. Fine, and T. Takahashi (1995), Sea-air flux of CO_2 in the North Pacific using shipboard and satellite data, *J. Geophys. Res.*, *100*(C7), 13,571–13,583.

Stocker, T. F., et al. (2013), IPCC, 2013: Climate change 2013: The physical science basis, contribution of working group i to the fifth assessment report of the intergovernmental panel on climate change, *Tech. Rep.*, Cambridge Univ. Press, U. K., and New York, doi:10.1017/CBO9781107415324.

Sverdrup, H. U., M. W. Johnson, and R. H. Fleming (1942), *The Oceans: Their Physics, Chemistry, and General Biology*, vol. 1087, Prentice-Hall, New York.

Takahashi, T., J. Olafsson, J. G. Goddard, D. W. Chipman, and S. C. Sutherland (1993), Seasonal variation of CO_2 and nutrients in the high-latitude surface oceans: A comparative study, *Global Biogeochem. Cycles*, *7*(4), 843–878, doi:10.1029/93GB02263.

Telszewski, M., X. A. Padín, and A. F. Ríos (2009), Estimating the monthly pCO_2 distribution in the North Atlantic using a self-organizing neural network, *Biogeosciences*, *6*(8), 1405–1421.

Thomas, H., and B. Schneider (1999), The seasonal cycle of carbon dioxide in Baltic Sea surface waters, *J. Mar. Syst.*, *22*(1), 53–67, doi:10.1016/S0924-7963(99)00030-5.

Tsunogai, S., S. Watanabe, and T. Sato (1999), Is there a continental shelf pump for the absorption of atmospheric CO_2?, *Tellus B*, *51*(3), 701–712.

Wanninkhof, R., et al. (2013), Global ocean carbon uptake: Magnitude, variability and trends, *Biogeosciences*, *9*(8), 10,961–11,012, doi:10.5194/bg-10-1983-2013.

Wesslander, K. (2011), The carbon dioxide system in the Baltic Sea surface waters, PhD thesis, Univ. of Gothenburg, Göteborg, Sweden.

Wollast, R. (1998), Evaluation and comparison of the global carbon cycle in the coastal zone and in the open ocean, *Sea*, *10*, 213–252.